ACS OMEGA

Open Access

http://pubs.acs.org/journal/acsodf

Article

High-Sensitivity Flexible Capacitive Pressure Sensors Based on Biomimetic Hibiscus Flower Microstructures

Ronghua Lan,[⊥] Jinyong Zhang,[⊥] Jing Chen, Wei Tang, Qingyang Wu, Xiaolin Zhou, Xiaoyang Kang, Jue Wang,* Hongbo Wang,* and Hui Li*

Cite This: *ACS Omega* 2024, 9, 13704−13713

Read Online

ACCESS | Metrics & More | Article Recommendations

ABSTRACT: The integration of low-dimensional nanomaterials with microscale architectures in flexible pressure sensors has garnered significant interest due to their outstanding performance in healthcare monitoring. However, achieving high sensitivity across different magnitudes of external pressure remains a critical challenge. Herein, we present a high-performance flexible pressure sensor crafted from biomimetic hibiscus flower microstructures coated with silver nanowires. When compared with a flat electrode, these microstructures as electrodes display significantly enhanced sensitivity and an extended stimulus−response range. Furthermore, we utilized an ionic gel film as the dielectric layer, resulting in an enhancement of the overall performance of the flexible pressure sensor through an increase in interfacial capacitance. Consequently, the capacitive pressure sensor exhibits an extraordinary ultrahigh sensitivity of 48.57 $[Kpa]^{-1}$ within the pressure range of 0−1 Kpa, 15.24 $[Kpa]^{-1}$ within the pressure range of 1−30 Kpa, and 3.74 $[Kpa]^{-1}$ within the pressure range of 30−120 Kpa, accompanied by a rapid response time (<58 ms). The exceptional performance of our flexible pressure sensor serves as a foundation for its numerous applications in healthcare monitoring. Notably, the flexible pressure sensor excels not only in detecting subtle physiological signals such as finger and wrist pulse signals, vocal cord vibrations, and breathing intensity but also demonstrates excellent performance in monitoring higher pressures, such as plantar pressure. We foresee that this flexible pressure sensor possesses significant potential in the field of wearable electronics.

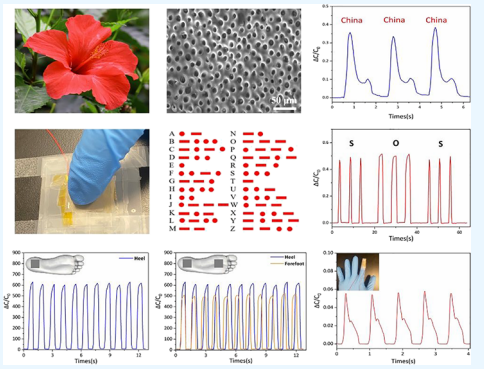

1. INTRODUCTION

In recent years, spurred by the advancements in material synthesis and processing technologies, flexible pressure sensors have increasingly seized the spotlight due to their remarkable integration, lightweight, and surface adaptability, particularly within the realm of medical monitoring.[1−3] Their implementation offers patients a safer and more comfortable means of monitoring their health status.[4] The human skin surface, known for its intricate and irregular topography, presents a plethora of potential applications for flexible pressure sensors,[5] encompassing crucial metrics like blood pressure,[6,7] heart rate,[8,9] respiratory rate,[10−12] pulse beat,[13−15] intracranial pressure,[16,17] intraocular pressure,[18,19] and external pressures including gait analysis,[20−22] tactile perception,[23,24] and speech recognition.[25−27] These applications demonstrate the immense potential of flexible pressure sensors in the field of medical monitoring. Flexible pressure sensors typically employ four primary sensing mechanisms: piezoresistive, capacitive, piezoelectric, and triboelectric.[28] Among these, capacitive pressure sensors offer notable advantages in terms of their rapid response, stability, and minimal susceptibility to environmental temperature variations.[29] Consequently, they have witnessed widespread utilization in both scientific research and practical applications. However, in order to meet comprehensive healthcare monitoring needs from detecting subtle heartbeats to gait pressures, it is necessary to develop low-cost manufacturing methods that can simultaneously achieve a wide dynamic range and ultrahigh sensitivity flexible pressure sensor.

Capacitive pressure sensors, which convert pressure input into changes in capacitance, are commonly manufactured by placing a dielectric layer between two parallel electrodes. With the presence of an applied voltage, the electrodes accumulate opposite charges, resulting in the formation of a capacitor. The associated capacitance (C) can be described by the equation $C = \varepsilon_0\varepsilon_r A/d$, where ε_0 stands for the vacuum's permittivity, ε_r signifies the relative permittivity of the dielectric layer, A

Received: October 14, 2023
Revised: February 28, 2024
Accepted: March 6, 2024
Published: March 15, 2024

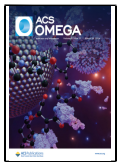

represents the shared area between the two electrodes, and d denotes the separation between the electrodes.[30] Utilizing an ionic gel film as the dielectric material with a high dielectric constant is considered one of the effective methods for enhancing the sensitivity of flexible pressure sensors.[31] The ionic gel film consists of ionic liquid fused with an elastomer. Ionic gel film has excellent electrical conductivity and good flexibility, which can meet the high flexibility requirements of flexible pressure sensors. When an ionic gel film is employed as the dielectric layer, the ions within the material will create a double electric layer in response to the influence of an electric field. Many double layers greatly improve the interface capacitance of flexible pressure sensor, thus significantly improving the sensitivity of sensor and other important performance. However, it is worth noting that under high-pressure conditions, the effectiveness of ionic gel film in enhancing the sensitivity flexible pressure sensor significantly diminishes.

Using flexible electrodes adorned with microstructures is another established approach to substantially enhance the sensitivity of flexible pressure sensors.[32] In general, various microstructures, including pyramids,[33] porous structures,[34,35] and polymeric pillars have been shown to exhibit significant deformations even under minor stimuli. For instance, Yang et al. showcased highly sensitive flexible pressure sensors, which were fabricated using a dielectric elastomer with a porous pyramid structure.[36] These porous pyramid microstructures exhibit a low compressive module, making them easily deformable under pressure, resulting in a change in capacitance. This ease of deformation is due to the large voids and interconnectivity within the porous pyramid microstructure, which allow for a greater degree of deformation compared to the flat structure. Moreover, the pyramid microstructures further enhance the sensitivity of the flexible pressure sensors. This occurs due to the concentration of applied stress at the apex of the pyramid, which effectively decreases the compressive modulus and leads to a more significant deformation. Consequently, this results in an increased sensitivity of the flexible pressure sensors. In addition, to investigate more novel microstructures in improving sensitivity, other molds have been investigated for replicating microstructures, including those inspired by plant leaves,[37] petals,[38] silk, sandpaper,[39] and more. In general, to achieve ultrahigh sensitivity and board range of the flexible sensor for various applications, microstructures are usually designed to be sharper and finer. For instance, the microstructures mimicked from silk or sandpaper, which are sharper and finer, can significantly improve the sensitivity of flexible pressure sensors due to their ability to deform easily under pressure. There exists a balance between sensitivity and sensing range. Microstructures based flexible pressure sensors often quickly saturate under small pressures, limiting their range (>50 Kpa). Hence, designing flexible pressure sensors capable of simultaneously achieving high sensitivity and a wide sensing range continues to be a significant challenge in market applications.

Herein, we present a straightforward method for manufacturing a highly sensitive flexible pressure sensor by incorporating biomimetic hibiscus flower microstructure (BHFM) and ionic gel film into the sensor. Traditional microstructures, such as micropyramids, microhemispheres, etc., typically need high-precision 3D printing, SEM or E-beam to fabricate, which are expensive and not easily accessible. This study introduces for the first time the use of biomimetic hibiscus flowers for the fabrication of microstructures. Compared to these microstructures, BHFM offers the advantages of simple fabrication, easy access, and low-cost. Finite element analysis results demonstrate that when the flexible pressure sensor is subjected to external forces, the sensor based on BHFM effectively increases the contact area between the two electrodes and plays an essential role in enhancing the sensor's compressibility. Our design effectively escalates the flexible pressure sensor's sensitivity by reducing the distance between two electrodes and broadening its sensing range, optimizing its overall performance. Furthermore, under the influence of electric field, the ionic gel film generates a substantial unit-area capacitance, forming an electrical double layer (EDL).[40] Both BHFM and EDL play essential roles in improving the sensitivity of the flexible pressure sensor and are particularly suitable for detecting subtle pressure variations. The fabricated capacitive pressure sensor exhibits remarkable performance with ultrahigh sensitivity of 48.57 $[\mathrm{Kpa}]^{-1}$ within the low-pressure range of 0−1 Kpa, 15.24 $[\mathrm{Kpa}]^{-1}$ within the pressure range of 1−30 Kpa, and 3.74 $[\mathrm{Kpa}]^{-1}$ within the pressure range of 30−120 Kpa, a rapid response time (<58 ms), low detection limit (5.5 mg), and excellent stability over 3000 cycles. These beneficial advantages allow for the utilization of this flexible pressure sensor for recording and identifying faint finger pulse signals during exercising. Finally, the flexible pressure sensor can be employed for high-pressure applications, such as plantar pressure, further showcasing its wide sensing range and suitability for medical monitoring.

2. EXPERIMENTAL SECTION

2.1. Materials. Polydimethylsiloxane (PDMS) elastomer and its accompanying curing agent were obtained from Dow Corning. Polyvinylidene fluoride-hexafluoropropylene copolymer (P(VDF-HFP)) and 1-ethyl-3-methylimidazolium bis-(trifluoromethylsulfonyl) imide ([EMIM][TFSI]) were procured from Sigma-Aldrich. AgNWs solution was provided by XFNANO Materials Tech Co. Ltd. TP silver paste with a weight of 500g was purchased from Nano Top.

2.2. Fabrication of Flexible Electrodes with Microstructure. Throughout the stages of preparation, performance characterization, and application demonstration experiments, the laboratory environment was set and maintained at 25 °C and a humidity level of 40%, aiming to more effectively avoid the potential influence of external factors on our flexible pressure sensor performance. First, the fresh hibiscus flower was immersed and rinsed in deionized water for a duration of 3 min and gently wipe-dried using Kimwipes; and then the flower edge was cut away as a rectangle piece to ensure uniformity in the surface microcones. Utilize tape to secure the hibiscus flower within the Petri dish, avoiding excessive pressure that could potentially harm the surface microstructure of the petal. The PDMS base and curing agent are thoroughly mixed at a weight ratio of 10:1 and then poured onto the hibiscus flower until completely submerged. Allow the PDMS to solidify by leaving it at room temperature for 48 h and then peel it off to use as a template for the second molding process. To achieve a more accurate replication of the microstructure, it was essential to increase the viscosity of the mold surface. The PDMS molding template was treated by plasma cleaner for 3 min, followed by a 30 min immersion in anhydrous ethanol under vacuum condition. Pour the previously prepared PDMS

https://doi.org/10.1021/acsomega.3c08044
ACS Omega 2024, 9, 13704−13713

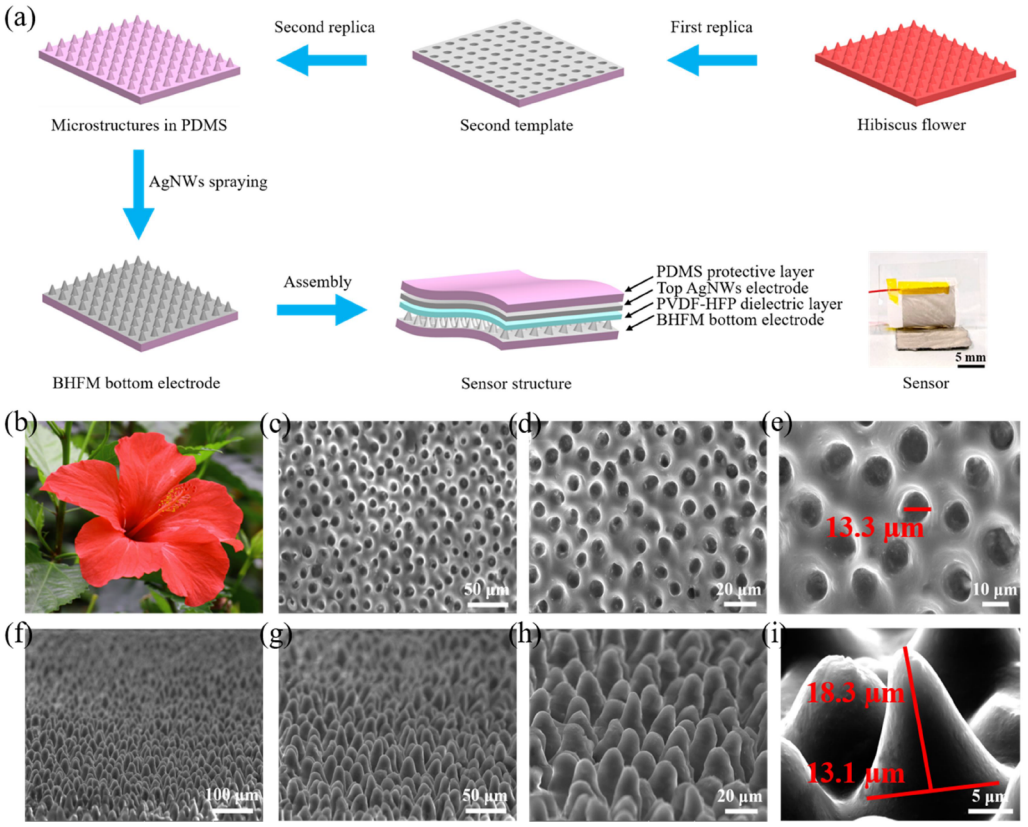

Figure 1. Fabrication of the capacitive pressure sensors. (a) Schematic depiction of the manufacturing procedure for the flexible pressure sensor utilizing BHFM as the basis. (b) Photograph of hibiscus flowers. (c–e) SEM images from a top-down perspective of microstructure caves. (f–h) SEM images from a 45° tilt perspective of the BHFM. (i) SEM image from a frontal perspective of the BHFM.

onto the second template and then evenly spin-coat it. Place it in an 80 °C oven for 1 h to cure and then peel off a 200 μm thick microstructured PDMS film from the second template. The AgNW solution was mixed with anhydrous ethanol in a 1:5 volume ratio, followed by 10 min of ultrasonic treatment to ensure thorough mixing. Subsequently, the PDMS substrate underwent a 1 min plasma treatment to enhance the adhesion capability of the membrane surface. The spray gun tip is 0.3 mm caliber, and the spray pressure is 25 psi with a distance of approximately 10 cm for fabricating the electrode layer of the flexible pressure sensor, ensuring its spray range covers the entire electrode and contributes to a certain level of uniformity. Finally, the electrode layer was placed in an 80 °C oven for about 3 h to evaporate the excess ethanol. Simultaneously, the thickness of the AgNW electrode does not affect its resistance, maintaining a consistent resistance level of approximately 2 Ω.

2.3. Fabrication of Ionic Gel Films and Assembly of the Pressure Sensor. The P(VDF-HFP) was mixed with acetone in a mass ratio of 1:7 and stirred at 60 °C using a magnetic stirrer for 2 h to ensure thorough mixing. Subsequently, 1 g of [EMIM][TFSI] was added to the PVDF-HFP/acetone mixed solution and stirred at room temperature for 2 h. The mixed solution was spin-coated onto a clean glass substrate at a speed of 400 rpm for 40 s, followed by annealing at 60 °C in a vacuum oven for 1 h to completely remove residual solvents from the ionic gel film. The prepared ionic gel film was peeled off and used as a dielectric layer. Finally, the BHFM based flexible pressure sensor was encapsulated with the microstructured AgNW electrode layer, the PVDF-HFP dielectric layer, and the AgNWs electrode layer, respectively, from bottom to top. The flexible pressure sensor has an overall square shape with a side length of approximately 1.5 cm, Figure 1a illustrates the manufacturing process and structural composition of the flexible pressure sensor.

2.4. Characterization. The micromorphology of BHFM was obtained through scanning electron microscopy. A force gauge (MS-05, Mark-10) and a vertically movable motorized test stand (ESM303, Mark-10) were used to apply external pressure onto the BHFM based flexible pressure sensor for the pressure characterization test. The recorded pressure data from the force gauge were transmitted to a laptop using a customized LabVIEW program. Simultaneously, the capacitance changes from the applied pressure were obtained by an impedance analyzer (SSA3032X, KEYSIGHT) under an AC voltage of 1 V at 1 kHz. By combining the obtained pressure and capacitance data, performance parameters such as sensor sensitivity, response time, detection limit, cyclicality, and stability were derived through data processing using Origin software.

3. RESULTS AND DISCUSSION

A photograph of a fresh hibiscus flower is shown in Figure 1a. After the first templating, we obtained relatively regular microstructure caves, as shown in the scanning electron microscopy (SEM) image of Figure 1c–e. The calculated average diameter of these microstructure caves is approximately 13.3 μm. Following the second templating, we fabricated microcones with an average diameter of approximately 13.1 μm and a height of approximately 18.3 μm, as

https://doi.org/10.1021/acsomega.3c08044
ACS Omega 2024, 9, 13704−13713

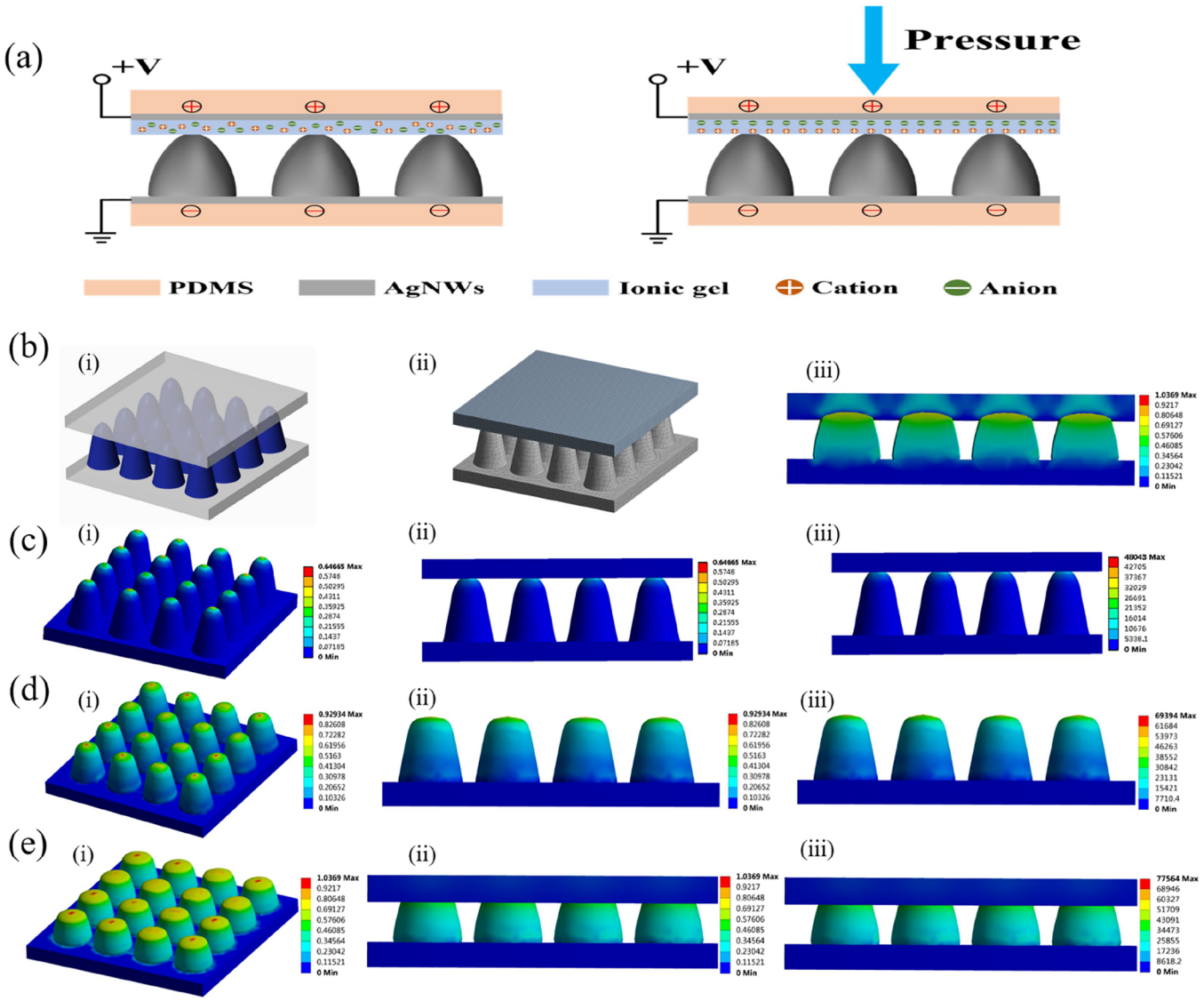

Figure 2. (a) Schematic representation of the sensing mechanism employed in the flexible pressure sensor with compressible microstructure. (b) Finite element simulation illustrated the press distribution of the pressure sensor under external forces. (c) Stress of BHFM under weak strain and pressure. (d) Stress of BHFM under medium strain and pressure. (e) Stress of BHFM under high strain and pressure.

shown in Figure 1f–i. The fabrication of electrode based on BHFM is critical for sensor. Spray-coating metal nanowires on the flexible substrate is a common method for preparing flexible electrodes. However, it is important to note that during multiple cycles of stretching or compressing, the electrodes may develop cracks, potentially leading to reduced conductivity. AgNWs, with their notable flexibility and ability to maintain superior electrical conductivity even after multiple compressions,[29] are frequently utilized as flexible electrode materials. In this work, AgNWs were used as the conductive layer on the smooth and microstructured PDMS substrate.

When the capacitive pressure sensor is subjected to external force, the internal structure is deformed, leading to a change in the distance between the two electrode layers and consequently causing a variation in capacitance. The working mechanism is plotted in Figure 2a. The flexible pressure sensor based on BHFM and an ionic gel film play a crucial role in enhancing key performance parameters. As shown in Figure 2a, under the influence of external pressure and an electric field, ions within the ionic gel film lead to the formation of an EDL at the electrode-ionic gel film interface. Initially, only a limited number of microcones in the electrode layer make contact with the ionic gel film, resulting in a relatively small contact area, consequently lower initial capacitance. With increasing external pressure, more microcones come into contact with the ionic gel film, effectively increasing the contact area between the two electrodes. This mechanism results in a substantial increase in the EDL capacitance of the flexible pressure sensor, further increasing its sensitivity. In other words, by generating EDL in the flexible pressure sensor, the ion transport performance and the sensitivity of the sensor are greatly improved. The response of the flexible pressure sensor primarily relies on the quantity of microcones in contact with the electron film and the contact area between the two electrode layers. To further comprehend the influence of biomimetic microstructures on sensor performance, finite element analysis (FEA) was employed to simulate the morphology of BHFM under weak, medium, and high strains and stresses as shown in Figure 2b–e. According to the capacitance calculation formula, $C = \varepsilon_0\varepsilon_r A/d$, where ε_0 stands for the vacuum's permittivity, ε_r signifies the relative

https://doi.org/10.1021/acsomega.3c08044
ACS Omega 2024, 9, 13704–13713

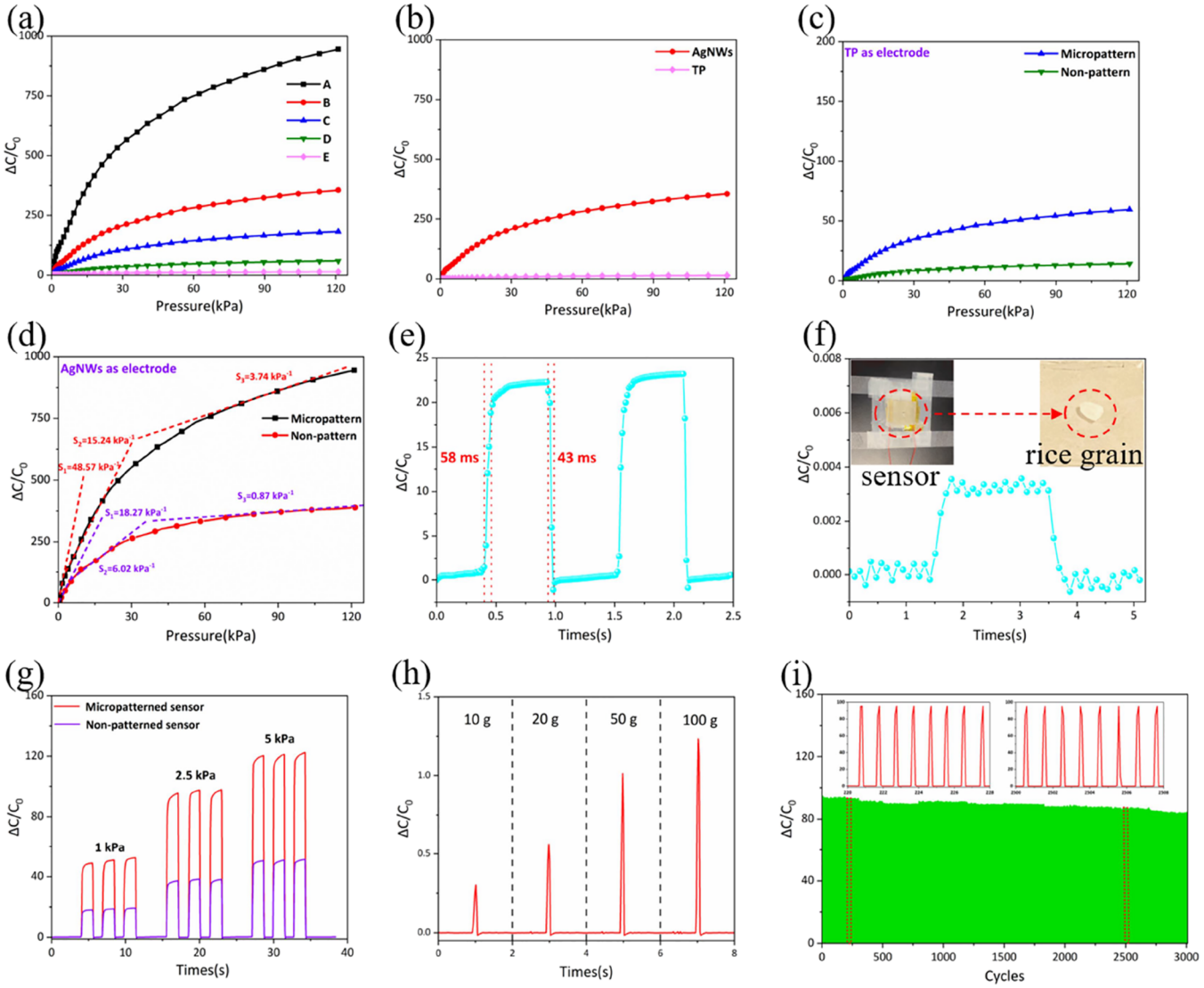

Figure 3. (a) Pressure variation of sensor capacitance based on different electrode materials and bionic microstructures. (b) AgNWs and TP silver paste were used as electrode materials, respectively, and compared the performance of flexible pressure sensors. (c) TP silver paste was used as electrode material and verified the effect of biomimetic microstructure on flexible pressure sensor. (d) The black and red curves represent the sensitivity of micropatterned and nonpatterned sensor, respectively (e) The response and recovery time of BHFM-based flexible pressure sensor. (f) The flexible pressure sensor has a detection limit for an ultralow weight grain rice of 5.5 mg. (g) Repeated real-time responses to the pressure of 1, 2.5, and 5 Kpa for the micropatterned and nonpatterned sensor. (h) Capacitive response of flexible pressure sensor to different pressures. (i) Performance of the BHFM flexible pressure sensor under a repeated pressure impact of 2.5 Kpa for 3000 cycles.

permittivity of the dielectric layer, A represents the overlapping area between the two electrodes, and d denotes the separation between the electrodes. When the same external force is applied, the electrode layer with microcone structures, compared to a flat electrode layer, can generate more local stress with the ionic gel film. This results in a larger overlapping area (A) and a smaller separation distance (d), consequently yielding a higher capacitance and thus exhibiting higher sensitivity. In general, the BHFM is adept at effectively causing the distance change between the two electrodes, making a positive contribution to the sensor sensitivity and sensing range.

Here, we verify the effect on the flexible pressure sensor sensitivity by incorporating different electrode materials and introducing biomimetic microstructures into the electrode layer. At the same time, PVDF-HFP was used for the dielectric layer materials. Figure 3a illustrates the sensitivity of flexible pressure sensors employing various electrode materials and biomimetic microstructures. Plots A−E in the figure represent the flexible pressure sensors with AgNWs/PVDF-HFP/Micro-AgNWs, AgNWs/PVDF-HFP/AgNWs, TP/PVDF-HFP/Micro-AgNWs, TP/PVDF-HFP/AgNWs, and TP/PVDF-HFP/TP, respectively. The results indicate that, with the incorporation of silver nanowires (AgNWs) electrodes and bioinspired microstructures, the flexible capacitive pressure sensor demonstrated an ultrahigh sensitivity, achieving up to 48.57 $[\text{Kpa}]^{-1}$ within the pressure range of 0−1 Kpa. Due to the higher viscosity of TP silver paste, it cannot be sprayed onto the PDMS with bioinspired microstructures like AgNWs, but can only be prepared by scraping. Therefore, the resulting electrode layer has a flat surface without forming microstructures. We compared the sensitivity of flexible pressure sensors using silver nanowires and TP silver paste as electrode materials, as shown in Figure 3b. The results clearly indicate

https://doi.org/10.1021/acsomega.3c08044
ACS Omega 2024, 9, 13704−13713

Table 1. Comparison of Recently Reported Pressure Sensors and Their Performance Parameters

materials	Sensitivity ($[Kpa]^{-1}$)	response time (ms)	limit of detection	cycle	ref
Ecoflex/graphene	12.3	78		4000	41
PDMS/ITO/PET	44.5	98	170 Pa	>2000	42
PDMS/Ag/PVDF	7.7	10		8000	43
CNT/PU	0.94	39			44
PDMS/Ag	3.627	40	5 Pa		45
AgNWs/PVDF-HFP	37.8	<78	24 Pa	2000	46
rGO/PDMS	1.85	150	60 Pa	10,000	47
Cu/PDMS/CNPs	26.6		20 Pa	3000	48
Ag/PVDF/PDMS	30.2	25	0.7 Pa		49
PDMS/MWCNT	10.805		1 Pa		50
CNTs-TPU/PET	1.02	66	0.7 Pa	60,000	51
AgNWs/PVDF-HFP	48.57	<58	5.5 mg	>3000	Here

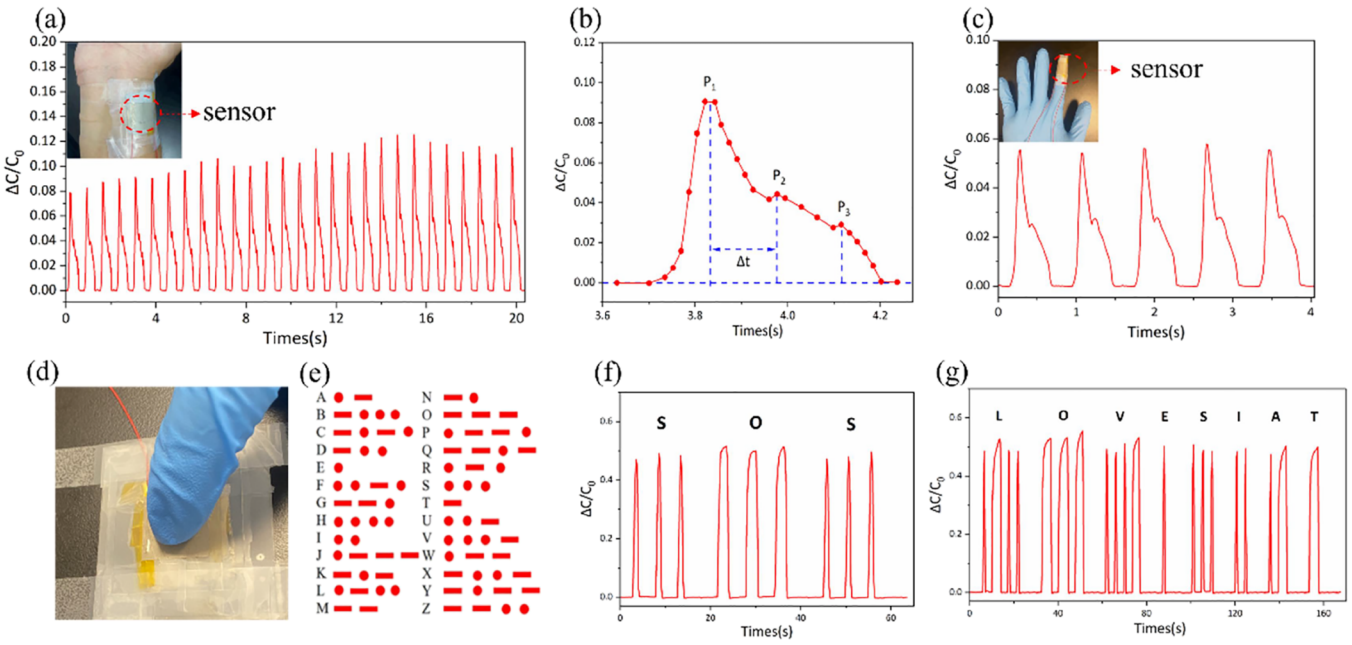

Figure 4. (a) Attaching the flexible pressure sensor to the wrist to monitor the arterial pulse of adult males. (b) Capturing a pulse wave from picture a, observe its peaks, and perform an analysis. (c) Attaching the flexible pressure sensor to the finger for monitoring finger pulses. (d) Pressing finger on the flexible pressure sensor and holding for different amounts of time. (e) Morse code table. (f, g) By pressing the finger onto the flexible pressure sensor, we can simulate the generation of Morse code, such as "SOS" and "LOVE SIAT".

that flexible pressure sensors using AgNWs as electrodes have significantly better sensitivity than those using TP silver paste. Due to the fact that the resistance of TP silver paste is approximately 10 times than that of AgNWs, the low resistance of AgNWs enhances the conductivity of the sensing process, thereby resulting in a higher sensitivity. Further, we chose TP silver paste as the top electrode and micropatterned and nonpatterned AgNWs as the bottom electrode, presented in Figure 3c. The results show that when biomimetic microstructures are introduced, the sensitivity of flexible pressure sensor increased by a factor of about 4.21. AgNWs is used as electrode materials, and the performance of biomimetic microstructure in flexible pressure sensor is studied, as shown in Figure 3d. It shows that the BHFM-based flexible capacitive pressure sensor exhibits ultrahigh sensitivity of 48.57 $[Kpa]^{-1}$ within the pressure range of 0−1 Kpa, 15.24 $[Kpa]^{-1}$ within the pressure range of 1−30 Kpa, and 3.74 $[Kpa]^{-1}$ within the pressure range of 30−120 Kpa. The electrode layer based on BHFM, owing to its finer and sharper morphology, undergoes rapid deformation when exposed to slight external forces, leading to an increase in the contact area between the two electrode layers and consequently exhibiting ultrahigh sensitivity. Furthermore, experimental testing revealed that the flexible pressure sensor has a response time of 58 ms and a recovery time of 43 ms, as shown in Figure 3e. Due to the ultrahigh sensitivity of the flexible pressure sensor in the low-pressure range, we attempted to place ultralightweight rice grain about 5.4×10^{-5} N on the sensor. Figure 3f depicts the transient response of the flexible pressure sensor when placing and removing rice grains, indicating a low detection limit (LOD) of 5.5 mg. To assess the repeatability of the flexible pressure sensor, tests were conducted at pressures of 1, 2.5, and 5 Kpa, as shown in Figure 3g. The results demonstrate that the BHFM-based flexible pressure sensor exhibits stable responses and excellent repeatability. The capacitance response of the flexible pressure sensor to different weights exhibited its good reliability as shown in Figure 3h. To assess the durability of the flexible pressure sensor, we applied repetitive pressure cycles to the sensor using a machine. Remarkably, even after 3000 cycles, the flexible pressure sensor exhibited excellent

https://doi.org/10.1021/acsomega.3c08044
ACS Omega 2024, 9, 13704−13713

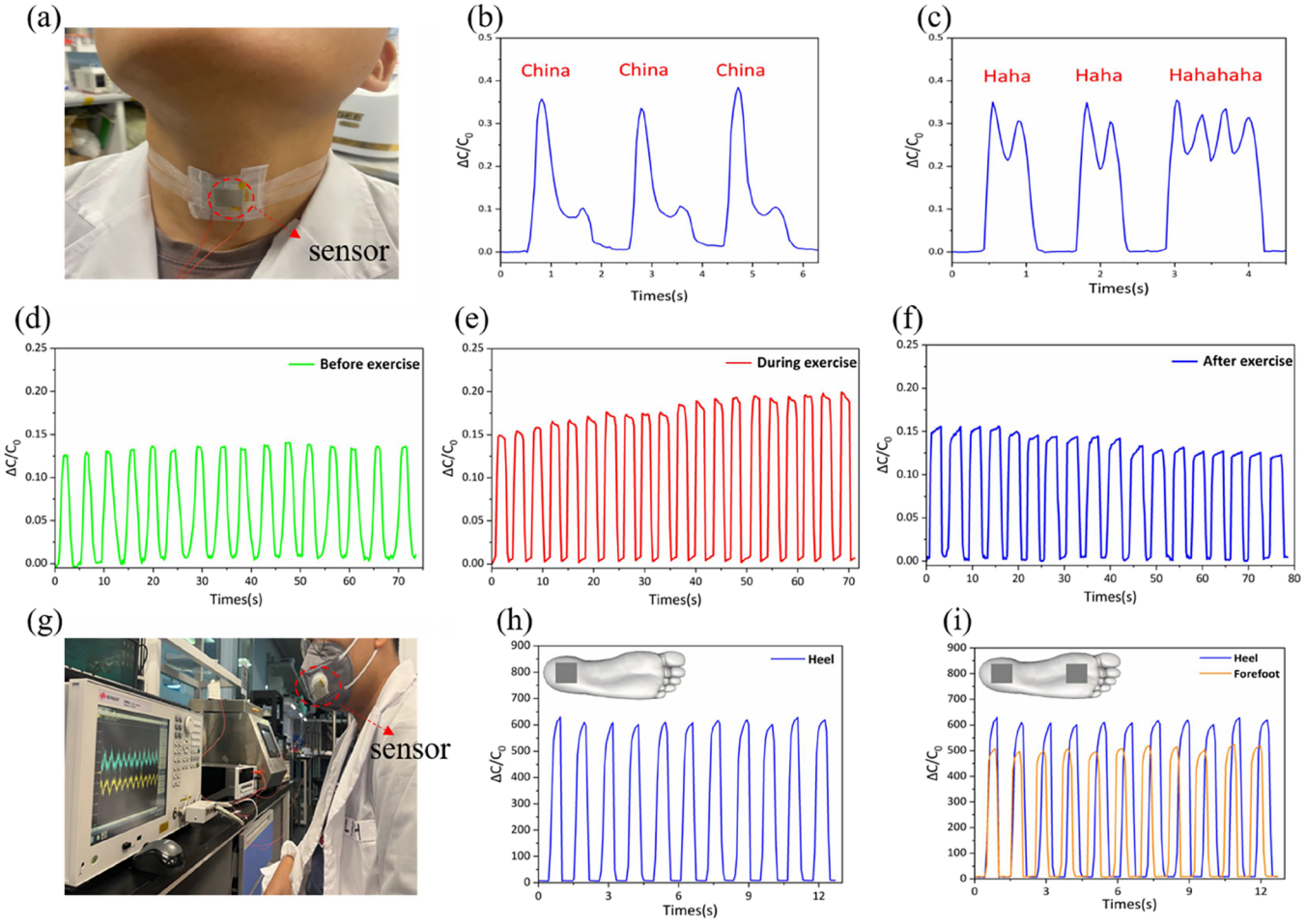

Figure 5. (a) Flexible pressure sensor attached to the throat and measuring the vibration signal emitted. (b) Subject pronounces the word "China". (c) Subject pronounces the word "haha" and "hahahaha". (d–f) Flexible pressure sensor measures the subject's breathing rate before, during and after exercise. (g) Flexible pressure sensor attached to the mask for respiration monitoring. (h) Attaching the flexible pressure sensor to the sole of the foot to monitor plantar pressure during walking. (i) Attaching the flexible pressure sensor separately to the heel and forefoot to monitor plantar pressure during walking.

stability, as shown in Figure 3i. The insets in the figure illustrate the sensor's capacitance response at different time intervals, further demonstrating that the flexible pressure sensor can consistently and stably detect pressure, meeting the requirements for prolonged health monitoring. Table 1 presents the key performance parameters of pressure sensors recently reported in the literature. From this comparison, it is evident that our fabricated capacitive pressure sensor, inspired by hibiscus flowers, exhibits high sensitivity and a rapid response time. These characteristics significantly enhance its potential for applications in the field of medical monitoring.

4. PRACTICAL APPLICATIONS FOR PHYSIOLOGICAL MONITORING AND MOVEMENT DETECTION

The flexible pressure sensor offers advantages such as high sensitivity, rapid response, and excellent stability. It can be used for monitoring human pulse and heart rate, contributing significantly to the early prevention of cardiovascular diseases. Figure 4a shows that the flexible pressure sensor was attached to a 23-year-old adult human wrist positioned above the radial artery. We can observe that within 20 s, the human showed 28 pulse waves, as shown in Figure 4a. After calculations, it was determined that his heart rate was about 84 beats per minute, which is in line with the heartbeat rate of a young, healthy person. However, most traditional flexible pressure sensors are unable to successfully capture the diastolic wave (P3) in the human pulse wave due to their low sensitivity. The BHFM-based flexible pressure sensor has high sensitivity, so it can clearly observe the pulse wave curve. We intercept a pulse wave, which consists of three distinct peaks, including a percussion wave (P1), tidal wave (P2), and diastolic wave (P3), as shown in Figure 4b. We can calculate the radial artery augmentation index (AIr = P2/P1), radial diastolic augmentation index (DAI = P3/P1), and the interval time (Δt) between P1 and P2 based on the pulse waveforms, which can be used as criteria for assessing arterial stiffness diagnoses.[52] The test subject's values of AIr, DAI, and Δt were 0.491, 0.321, and 0.176 s, respectively, which were consistent with the reference values of a 23-year-old healthy male.[53] Furthermore, most existing flexible pressure sensors cannot detect fingertip pulses, but our BHFM flexible pressure sensor with high sensitivity makes it a good choice for fingertip pulse monitoring. The monitoring of fingertip pulse signal can be simply realized by attaching flexible pressure sensor on the center of a fingertip surface and recording the capacitance signals and presenting the corresponding pulse signals as shown in Figure 4c. The results demonstrate that our flexible pressure sensor on a fingertip can acquire stable pulse signals. This is a reference

https://doi.org/10.1021/acsomega.3c08044
ACS Omega 2024, 9, 13704−13713

chart for Morse code, which uses dots and dashes to represent various letters in the alphabet, as shown in Figure 4e. As demonstrated in Figure 4d, by lightly pressing one's fingers on the flexible pressure sensor, short presses and long presses correspond to a dot and a dash, respectively. The signal waveform obtained from the sensor's output can be used to simulate the generation of Morse code. For example, a "S" is generated by three dots on the flexible pressure sensor, a "O" is generated by three dashes and then three more dots, and finally a "SOS" is generated. The Morse code "LOVE SIAT" is also generated in this way, depicted in Figure 4f,g. The flexible pressure sensor could be used as an encrypted information generating and sending device.

The flexible pressure sensor was affixed to the vocal folds of the subject's throat to measure weak vibration signals emitted during speech as shown in Figure 5a−c. During the testing process, subject was instructed to produce the same vocalizations as consistently as possible. When subject pronounced "China", the word's requirement for consecutive enunciation of "Chi" and "na" syllables resulted in the output signal displaying two distinct peaks, as shown in Figure 5b. Similarly, when pronouncing "haha", composed of two identical syllables, two nearly identical peaks were observed. This pattern extended to "hahahaha", generating four nearly identical signal peaks, as shown in Figure 5c. The result shows the same word corresponds to almost the same waveform, which verifies accuracy and reliability of our flexible pressure sensor. The flexible pressure sensor was affixed to a facemask that monitors user's breathing in different movements and was presented in Figure 5g. The flexible pressure sensor successfully detected the subject's breathing intensity during different states of movement, as shown in Figure 5d−f. Our in-depth analysis of the subject's respiratory waveforms during various physical activities revealed changes in breathing rates, with 13, 17, and 14 breaths per minute recorded before, during, and after exercise, respectively, which indicated the body's varying oxygen needs. During exercise, the increased oxygen demand led to more intense and faster breathing, as clearly reflected in the plot, with a notable increase in waveform amplitude. This adjustment in breathing, accurately captured by our flexible pressure sensor, indicates the body's automatic response to fulfill increased oxygen needs. After exercise, although the breathing rate and intensity decrease to restore normalcy, they remain higher than at rest, promoting faster carbon dioxide expulsion and recovery. This noninvasive monitoring method provides vital insights into respiratory changes during different physical states and offers valuable data for early diagnosis of respiratory diseases. The flexible pressure sensor also has the capability to detect high pressures, and in this study, we employ it for monitoring plantar pressure. In daily activities, continuous pressure is generated on the soles of our feet. In the walking phase, extremely stable and uniform waveforms are exhibited by the output signal from a flexible pressure sensor, which is attached to the heel and presented in Figure 5h. Furthermore, by installing two flexible pressure sensors at the soles of the shoes, the heel strike and forefoot strike can be accurately detected throughout the walking process, as shown in Figure 5i. The flexible pressure sensor can effectively identify motion postures and has great potential for gait monitoring. Not only that, but also it can monitor and understand daily gaits and walking patterns, providing important information about body posture and movement issues; thereby contributing to guidance of daily exercises, rehabilitation therapy, and physical therapy treatment plans, as well as the evaluation of treatment effects.

5. CONCLUSIONS

In this work, we prepared a flexible capacitive pressure sensor with ultrahigh sensitivity and a wide working range by incorporating BHFM into the electrode layer and employing an ionic gel film as the dielectric layer. The flexible pressure sensor shows that its ultrahigh sensitivity is 48.57 $[\mathrm{Kpa}]^{-1}$ within the pressure range of 0−1 Kpa, 15.24 $[\mathrm{Kpa}]^{-1}$ within the pressure range of 1−30 Kpa, and 3.74 $[\mathrm{Kpa}]^{-1}$ within the pressure range of 30−120 Kpa, accompanied by a rapid response time (<58 ms). Moreover, the flexible pressure sensor also presents a low LOD of 5.5 mg, and high stability over 3000 cyclic loading. The flexible capacitive pressure sensor, characterized by its high sensitivity, rapid response, and wide working range, can be employed for monitoring pulse signals, vocal cord vibrations, respiratory intensity, and gait analysis. Overall, the BHFM-based capacitive pressure sensor shows significant promise for applications in medical monitoring and is positioned to play an important role in human-computer interaction.

AUTHOR INFORMATION

Corresponding Authors

Jue Wang − *Key Laboratory of Biomedical Information Engineering of Ministry of Education, School of Life Science and Technology, Institute of Health and Rehabilitation Science, Xi'an Jiaotong University, Xi'an 710049 Shaanxi, China*; Email: juewang_xjtu@126.com

Hongbo Wang − *Institute of AI and Robotics, Academy for Engineering and Technology, Fudan University, Shanghai 200433, China*; Email: Wanghongbo@fudan.edu.cn

Hui Li − *College of Big Data and Internet, Shenzhen Technology University, Shenzhen 518118 Guangdong, China; Shenzhen Institute of Advanced Technology, Chinese Academy of Sciences, Shenzhen 518055 Guangdong, China*; orcid.org/0000-0002-7245-9609; Email: lihui2@sztu.edu.cn

Authors

Ronghua Lan − *College of Big Data and Internet, Shenzhen Technology University, Shenzhen 518118 Guangdong, China; Shenzhen Institute of Advanced Technology, Chinese Academy of Sciences, Shenzhen 518055 Guangdong, China*

Jinyong Zhang − *College of Big Data and Internet, Shenzhen Technology University, Shenzhen 518118 Guangdong, China*

Jing Chen − *Shenzhen Institute of Advanced Technology, Chinese Academy of Sciences, Shenzhen 518055 Guangdong, China*

Wei Tang − *Shenzhen Institute of Advanced Technology, Chinese Academy of Sciences, Shenzhen 518055 Guangdong, China*

Qingyang Wu − *College of Big Data and Internet, Shenzhen Technology University, Shenzhen 518118 Guangdong, China*

Xiaolin Zhou − *College of Big Data and Internet, Shenzhen Technology University, Shenzhen 518118 Guangdong, China*

Xiaoyang Kang − *Institute of AI and Robotics, Academy for Engineering and Technology, Fudan University, Shanghai 200433, China*

Complete contact information is available at: https://pubs.acs.org/10.1021/acsomega.3c08044

https://doi.org/10.1021/acsomega.3c08044
ACS Omega 2024, 9, 13704−13713

Author Contributions

[⊥]R.L. and J.Z. contributed equally to this work.

Notes

The authors declare no competing financial interest.

■ ACKNOWLEDGMENTS

This research was partially supported by National Natural Science Foundation of China (U1913216, 31972907, 32071346, and 32271403), Founding Program for Self-Developing Instruments and Equipment of Shenzhen Technology University (No. JSZZ202301007).

■ REFERENCES

(1) Min, S. W.; Kim, D. H.; Joe, D. J.; et al. Clinical Validation of a Wearable Piezoelectric Blood-Pressure Sensor for Continuous Health Monitoring. *Adv. Mater.* **2023**, *35*, No. e2301627.
(2) Chang, K. B.; Parashar, P.; Shen, L. C.; et al. A triboelectric nanogenerator-based tactile sensor array system for monitoring pressure distribution inside prosthetic limb. *Nano Energy* **2023**, *111*, No. 108397.
(3) Yao, S.; Ren, P.; Song, R.; et al. Nanomaterial-Enabled Flexible and Stretchable Sensing Systems: Processing, Integration, and Applications. *Adv. Mater.* **2019**, *32*, No. 1902343.
(4) Li, L.; Cheng, Y. F.; Cao, H. H.; et al. MXene/rGO/PS spheres multiple physical networks as high-performance pressure sensor. *Nano Energy* **2022**, *95*, No. 106986.
(5) Lee, Y.; Ahn, J.-H. Biomimetic Tactile Sensors Based on Nanomaterials. *ACS Nano* **2020**, *14* (2), 1220−1226.
(6) Ouyang, H.; Li, Z.; Gu, M.; et al. A Bioresorbable Dynamic Pressure Sensor for Cardiovascular Postoperative Care. *Adv. Mater.* **2021**, *33*, No. 2102302.
(7) Chen, S.; Wu, N.; Lin, S.; et al. Hierarchical Elastomer Tuned Self-powered Pressure Sensor for Wearable Multifunctional Cardiovascular Electronics. *Nano Energy* **2020**, *70*, No. 104460.
(8) Kaisti, M.; Panula, T.; Leppanen, J.; et al. Clinical assessment of a non-invasive wearable MEMS pressure sensor array for monitoring of arterial pulse waveform, heart rate and detection of atrial fibrillation. *NPJ Digital Med.* **2019**, *2*, 39.
(9) Tang, X.; Wu, C.; Gan, L.; et al. Multilevel Microstructured Flexible Pressure Sensors with Ultrahigh Sensitivity and Ultrawide Pressure Range for Versatile Electronic Skins. *Small* **2019**, *15* (10), No. e1804559.
(10) Ghosh, R.; Song, M. S.; Park, J.; et al. Fabrication of piezoresistive Si nanorod-based pressure sensor arrays: A promising candidate for portable breath monitoring devices. *Nano Energy* **2021**, *80*, No. 105537.
(11) Yang, W.; Li, N.-W.; Zhao, S.; et al. A Breathable and Screen-Printed Pressure Sensor Based on Nanofiber Membranes for Electronic Skins. *Adv. Mater. Technol.* **2018**, *3* (2), No. 1700241.
(12) Zhong, J.; Li, Z.; Takakuwa, M.; et al. Smart Face Mask Based on an Ultrathin Pressure Sensor for Wireless Monitoring of Breath Conditions. *Adv. Mater.* **2022**, *34* (6), No. e2107758.
(13) Peng, B.; Zhao, F.; Ping, J.; et al. Recent Advances in Nanomaterial-Enabled Wearable Sensors: Material Synthesis, Sensor Design, and Personal Health Monitoring. *Small* **2020**, *16*, No. 2002681, DOI: 10.1002/smll.202002681.
(14) Yin, B.; Liu, X.; Gao, H.; et al. Bioinspired and bristled microparticles for ultrasensitive pressure and strain sensors. *Nat. Commun.* **2018**, *9* (1), 5161.
(15) Yi, J.; Xianyu, Y. Gold Nanomaterials-Implemented Wearable Sensors for Healthcare Applications. *Adv. Funct. Mater.* **2022**, *32*, No. 2113012.
(16) Shin, J.; Yan, Y.; Bai, W.; et al. Bioresorbable pressure sensors protected with thermally grown silicon dioxide for the monitoring of chronic diseases and healing processes. *Nat. Biomed. Eng.* **2019**, *3* (1), 37−46.
(17) Jiang, N.; Flyax, S.; Kurz, W.; et al. Intracranial Sensors for Continuous Monitoring of Neurophysiology. *Adv. Mater. Technol.* **2021**, *6* (12), No. 2100339.
(18) Liu, Z.; Wang, G.; Pei, W.; et al. Application of graphene nanowalls in an intraocular pressure sensor. *J. Mater. Chem. B* **2020**, *8* (38), 8794−8802.
(19) Kim, J.; Kim, J.; Ku, M.; et al. Intraocular Pressure Monitoring Following Islet Transplantation to the Anterior Chamber of the Eye. *Nano Lett.* **2020**, *20* (3), 1517−1525.
(20) Lin, Z.; Wu, Z.; Zhang, B.; et al. A Triboelectric Nanogenerator-Based Smart Insole for Multifunctional Gait Monitoring. *Adv. Mater. Technol.* **2019**, *4* (2), No. 1800360.
(21) Ahn, S.; Cho, Y.; Park, S.; et al. Wearable multimode sensors with amplified piezoelectricity due to the multi local strain using 3D textile structure for detecting human body signals. *Nano Energy* **2020**, *74*, No. 104932.
(22) Song, Z.; Li, W.; Bao, Y.; et al. Bioinspired Microstructured Pressure Sensor Based on a Janus Graphene Film for Monitoring Vital Signs and Cardiovascular Assessment. *Adv. Electron. Mater.* **2018**, *4* (11), No. 1800252.
(23) Niu, H. S.; Li, H.; Gao, S.; et al. Perception-to-Cognition Tactile Sensing Based on Artificial-Intelligence-Motivated Human Full-Skin Bionic Electronic Skin. *Adv. Mater.* **2022**, *34* (31), No. 2202622.
(24) Zhao, C.; Wang, Y. J.; Tang, G. Q.; et al. Ionic Flexible Sensors: Mechanisms, Materials, Structures, and Applications. *Adv. Funct. Mater.* **2022**, *32* (17), No. 2110417.
(25) Li, X.; Fan, Y. J.; Li, H. Y.; et al. Ultracomfortable Hierarchical Nanonetwork for Highly Sensitive Pressure Sensor. *ACS Nano* **2020**, *14* (8), 9605−9612.
(26) Li, Z.; Zhang, S.; Chen, Y.; et al. Gelatin methacryloyl-based tactile sensors for medical wearables. *Adv. Funct. Mater.* **2020**, *30* (49), No. 2003601.
(27) Liang, C.; Jiao, C. Y.; Gou, H. R.; et al. Facile construction of electrochemical and self-powered wearable pressure sensors based on metallic corrosion effects. *Nano Energy* **2022**, *104*, No. 107954.
(28) Liu, M.-Y.; Hang, C.-Z.; Zhao, X.-F.; et al. Advance on flexible pressure sensors based on metal and carbonaceous nanomaterial. *Nano Energy* **2021**, *87*, 106181.
(29) Chen, W. F.; Yan, X. Progress in achieving high-performance piezoresistive and capacitive flexible pressure sensors: A review. *J. Mater. Sci. Technol.* **2020**, *43*, 175−188.
(30) Ruth, S. R. A.; Feig, V. R.; Tran, H.; et al. Microengineering Pressure Sensor Active Layers for Improved Performance. *Adv. Funct. Mater.* **2020**, *30* (39), No. 2003491.
(31) Kim, K. L.; Cho, S. H.; Lee, J. B.; et al. Transparent and Flexible Graphene Pressure Sensor with Self- Assembled Topological Crystalline Ionic Gel. *ACS Appl. Mater. Interfaces* **2023**, *15* (15), 19319−19329.
(32) Wang, C.; Wang, C.; Huang, Z.; et al. Materials and Structures toward Soft Electronics. *Adv. Mater.* **2018**, *30*, No. 1801368.
(33) Ma, C.; Xu, D.; Huang, Y. C.; et al. Robust Flexible Pressure Sensors Made from Conductive Micropyramids for Manipulation Tasks. *ACS Nano* **2020**, *14* (10), 12866−12876.
(34) Zheng, X. H.; Zhang, S. L.; Zhou, M. J.; et al. MXene Functionalized, Highly Breathable and Sensitive Pressure Sensors with Multi-Layered Porous Structure. *Adv. Funct. Mater.* **2023**, *33*, No. 2214880.
(35) Song, R. Q.; Ren, P.; Liu, Y. X.; et al. Stretchable Organic Transistor Based Pressure Sensor Employing a Porous Elastomer Gate Dielectric. *Adv. Mater. Technol.* **2023**, *8*, No. 2202140.
(36) Yang, J. C.; Kim, J. O.; Oh, J.; et al. Microstructured Porous Pyramid-Based Ultrahigh Sensitive Pressure Sensor Insensitive to Strain and Temperature. *ACS Appl. Mater. Interfaces* **2019**, *11* (21), 19472−19480.
(37) Yao, G.; Xu, L.; Cheng, X. W.; et al. Bioinspired Triboelectric Nanogenerators as Self-Powered Electronic Skin for Robotic Tactile Sensing. *Adv. Funct. Mater.* **2020**, *30* (6), No. 1907312.

https://doi.org/10.1021/acsomega.3c08044
ACS Omega 2024, 9, 13704−13713

(38) Wan, Y. B.; Qiu, Z. G.; Huang, J.; et al. Natural Plant Materials as Dielectric Layer for Highly Sensitive Flexible Electronic Skin. *Small* **2018**, *14* (35), No. 1801657.
(39) Han, S. J.; Liu, C. R.; Huang, Z. B.; et al. High-Performance Pressure Sensors Based on 3D Microstructure Fabricated by a Facile Transfer Technology. *Adv. Mater. Technol.* **2019**, *4* (5), No. 1800640.
(40) Amoli, V.; Kim, J. S.; Kim, S. Y.; et al. Ionic Tactile Sensors for Emerging Human-Interactive Technologies: A Review of Recent Progress. *Adv. Funct. Mater.* **2019**, *30* (20), No. 1904532.
(41) Qi Wu, Y. Q.; Guo, R.; et al. Triode-Mimicking Graphene Pressure Sensor with Positive Resistance Variation for Physiology and Motion Monitoring. *ACS Nano* **2020**, *14* (8), 10104−10114.
(42) Chang, J.; Yang, J.-O. K.; Jinwon, O.; et al. Microstructured Porous Pyramid-based Ultra-high Sensitive Pressure Sensor Insensitive to Strain and Temperature. *ACS Appl. Mater. Interfaces* **2019**, *11* (21), 19272−19298.
(43) Lin, W.; Wang, B.; Peng, G.; et al. Skin-Inspired Piezoelectric Tactile Sensor Array with Crosstalk-Free Row+Column Electrodes for Spatiotemporally Distinguishing Diverse Stimuli. *Adv. Sci.* **2021**, *8* (3), No. 2002817.
(44) Lan, L.; Jiang, C.; Yao, Y.; et al. A stretchable and conductive fiber for multifunctional sensing and energy harvesting. *Nano Energy* **2021**, *84*, 105954.
(45) Lei, H.; Xiao, J.; Chen, Y.; et al. Bamboo-inspired self-powered triboelectric sensor for touch sensing and sitting posture monitoring. *Nano Energy* **2022**, *91*, No. 106670.
(46) Chen, J.; Li, L.; Zhu, Z.; et al. Bioinspired design of highly sensitive flexible tactile sensors for wearable healthcare monitoring. *Mater. Today Chem.* **2022**, *23*, No. 100718.
(47) Guan, H.; Meng, J.; Cheng, Z.; et al. Processing Natural Wood into a High-Performance Flexible Pressure Sensor. *ACS Appl. Mater. Interfaces* **2020**, *12* (41), 46357−46365.
(48) Zhong, M.; Zhang, L.; Liu, X.; et al. Wide linear range and highly sensitive flexible pressure sensor based on multistage sensing process for health monitoring and human-machine interfaces. *Chem. Soc. Rev.* **2021**, *412*, No. 128649.
(49) Xiong, Y.; Shen, Y.; Tian, L.; et al. A flexible, ultra-highly sensitive and stable capacitive pressure sensor with convex microarrays for motion and health monitoring. *Nano Energy* **2020**, *70*, No. 104436.
(50) Li, W.; Jin, X.; Han, X.; et al. Synergy of Porous Structure and Microstructure in Piezoresistive Material for High-Performance and Flexible Pressure Sensors. *ACS Appl. Mater. Interfaces* **2021**, *13* (16), 19211−19220.
(51) Yin, Y. M.; Li, H. Y.; Xu, J.; et al. Facile Fabrication of Flexible Pressure Sensor with Programmable Lattice Structure. *ACS Appl. Mater. Interfaces* **2021**, *13* (8), 10388−10396.
(52) Chu, Y.; Zhong, J.; Liu, H.; et al. Human Pulse Diagnosis for Medical Assessments Using a Wearable Piezoelectret Sensing System. *Adv. Funct. Mater.* **2018**, *28* (40), No. 1803413.
(53) Fu, Y.; Zhao, S.; Wang, L.; et al. A Wearable Sensor Using Structured Silver-Particle Reinforced PDMS for Radial Arterial Pulse Wave Monitoring. *Adv. Healthcare Mater.* **2019**, *8* (17), No. 1900633.

https://doi.org/10.1021/acsomega.3c08044
ACS Omega 2024, 9, 13704−13713